Design and optimization of torsion harvester of *Lycium barbarum* L.

Qingyu Chen, Shixia Zhang, Naishuo Wei, Puhang Li, Guangrui Hu, Jun Chen*, Yu Chen
(*College of Mechanical and Electronic Engineering, Northwest A & F University, Yangling 712100, Shaanxi, China*)

Abstract: The production of *Lycium barbarum* L. is a labor-intensive industry. Multiple manual harvests are required during the harvesting season, which contributes to the high harvesting costs. The cultivation conditions of *L. barbarum* were investigated to increase efficiency and mitigate harvesting damage. A torsion harvester was designed according to the characteristic of infinite inflorescence and the distribution of detachment force, and the kinematics model of the harvester was established. The vibration responses of ripe and unripe fruit were obtained through ADAMS simulation of the branch model, and the influencing factors and value range of the torsion harvester were also determined. The mathematical models of ripe fruit harvesting rate, unripe fruit harvesting rate, ripe fruit damage rate and torsion angle, vibration rods distance, and vibration frequency were established by the Box-Behnken test. The influences of various factors on ripe fruit harvesting rate, unripe fruit harvesting rate, and ripe fruit damage rate were analyzed, and the best parameter combination was obtained: torsion angle 73.66°, vibration rods distance 35.51 mm and vibration frequency 19.12 Hz. Field experiment showed that the harvesting rate of ripe fruit is 95.67%, the harvesting rate of unripe fruit is 4.68%, and the damage rate of ripe fruit is 3.70%. The research results can promote the mechanization process of *L. barbarum* harvest, and provide a reference for vibration harvest of berries.
Keywords: *L. barbarum*, vibrating, torsion, response surface method, parameters optimization, ADAMS, RSM
DOI: 10.25165/j.ijabe.20241704.8082

Citation: Chen Q Y, Zhang S X, Wei N S, Li P H, Hu G R, Chen J, et al. Design and optimization of torsion harvester of *Lycium barbarum* L. Int J Agric & Biol Eng, 2024; 17(4): 109–115.

1 Introduction

Lycium barbarum L. (*L. barbarum*) is an infinite inflorescence plant, with ripe fruit, unripe fruit, and flowers growing continuously in branch[1,2]. The production of *L. barbarum* is a labor-intensive business. The need for multiple manual harvests throughout the harvesting season contributes to the high cost of harvesting. In Ningxia China, *L. barbarum* is harvested every 7 d, and it should be harvested in time after maturity to prevent diseases from affecting fruit quality. Harvest time requires a lot of labor, and summer harvesting is affected by high temperatures and sunlight, making for difficult working conditions and low artificial harvesting efficiency. Therefore, it is critical to find a quick solution to the harvesting issue[3-5].

L. barbarum is seldom planted and distributed abroad, and most of the relevant studies are conducted in China[6-8]. The branches of *L. barbarum* are intertwined, the fruit is tender and fragile, the large-scale machinery has poor field passability, and it is challenging to realize mechanized harvesting quickly. These factors indicate that *L. barbarum*'s agronomy needs to be improved. At the same time, the existing harvester can easily cause fruit damage, thereby affecting the income[9-12]. Therefore, semi-mechanized harvesting has emerged as a workable concept at this stage, while the development of small-sized portable harvesting equipment has become a research hotspot, and achieving high-efficiency and low-loss harvesting has become a challenge. Zhang et al.[13] designed a portable vibrating harvester, which relies on inertia force to make the fruit fall off. However, the mechanical structure uses multi-point clamping branches to vibrate during harvest, and the direct fruit contact with the harvester can easily cause damage. Zhang et al.[14] designed a comb-brush harvester with variable spacing, which brushes the ripe fruit to make it fall off. However, the harvester needs to manually align the fruits, it is therefore less efficient than that of the vibratory harvester. Xu et al.[15] designed a harvester that combines vibrating and comb-brushing types, thus harvesting ripe fruit using two different methods. However, experimental results showed that the harvesting rate of unripe fruit is high. According to test results of different types of harvesters, the vibration harvesting method can effectively improve the harvesting efficiency, but the mechanical structure's restrictions make it difficult to increase the vibration frequency. The harvesting effect in vibration harvester is typically improved using a large amplitude or vibrating brush, but there are still some issues such as harvesting unripe fruits and damaging ripe fruits during the harvest[16-18]. This will affect the subsequent output and reduce the economic benefit, which is unacceptable to manufacturers.

According to the characteristics of infinite inflorescence of *L. barbarum* and the detachment force of fruit-flower-leaf-branch, a torsion harvester was designed using the vibration harvesting method, and the kinematics model of the harvester was established. To optimize the structure and working parameters of the harvester, the kinematics and dynamics simulation of the harvester was carried out through ADAMS. Then, based on response surface methodology (RSM), the effects of the torsion angle, vibration rods

Received date: 2023-12-13 **Accepted date:** 2024-05-29
Biographies: Qingyu Chen, PhD candidate, research interest: forest fruit harvesting machinery design, Email: 2019050914@nwafu.edu.cn; **Shixia Zhang**, MS candidate, research interests: forest fruit harvesting machinery design, Email: 1048912069@nwafu.edu.cn; **Naishuo Wei**, PhD candidate, research interest: intelligent agricultural equipment technology, Email: weinaishuo@nwafu.edu.cn; **Puhang Li**, MS candidate, research interest: image recognition, control algorithm, Email: xnlph@nwafu.edu.cn; **Guangrui Hu**, PhD candidate, research interest: Intelligent apple harvesting robot, Email: 2017050952@nwsuaf.edu.cn; **Yu Chen**, PhD, Associate Professor, research interest: intelligent agricultural machinery equipment and intelligent vehicle control, Email: jdxy73@nwafu.edu.cn.

***Corresponding author: Jun Chen**, PhD, Professor, research interest: intelligent agricultural equipment technology and vehicle performance testing. College of Mechanical and Electronic Engineering, Northwest A&F University, Yangling 712100, Shaanxi, China. Tel: +86-13572191773, Email: chenjun_jdxy@nwafu.edu.cn.

distance, and vibration frequency on the harvesting rates of ripe and unripe fruits, as well as on the damage rate of ripe fruit were determined. Field experiments were used to obtain and validate the optimized parameters.

2 Materials and methods

2.1 Biological characteristics of *L. barbarum*

The fundamental idea behind vibration harvesting is to transfer kinetic energy to fruit branches, and produce a detachment force at the junction where the fruit and the fruit handle meet, causing the fruit to fall off[19]. Numerous studies on vibration harvesting of olive, coffee, and camellia fruit have been conducted recently[20-23]. However, as shown in Figure 1, it is necessary to avoid damaging ripe fruits and harvesting unripe fruits due to the vulnerable ripe fruit and infinite inflorescence of *L. barbarum*.

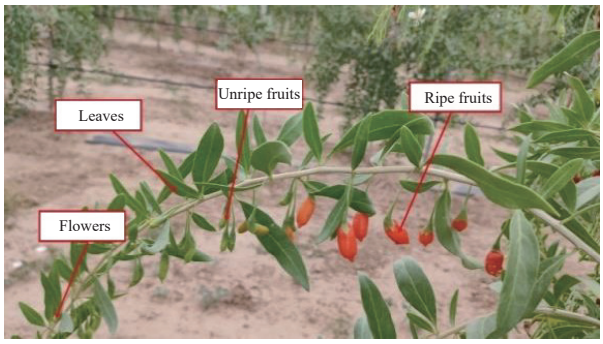

Figure 1 Characteristics of infinite inflorescence of *L. barbarum*

To discover the growth characteristics of *L. barbarum*, this study investigates the harvest and planting in Ningxia Zhengqihong *L. barbarum* Industry Development Co., Ltd., Gangou Village, Sanying Town, Yuanzhou District, Guyuan City, Ningxia Hui Autonomous Region (36°17′32.9″N, 106°6′41.5″E). The "Ningqi 7" variety under investigation had shrubs that were 3-4 years old. The shrubs were artificially pruned into standardized hedge cultivation mode; the height of shrubs is 1.1-2.4 m, the planting row spacing is 3 m, and the distance between shrubs is 1.1 m. The detachment force was measured, as shown in Table 1. The results showed that there was a clear distinction in the detachment force between ripe fruit, unripe fruit, flowers, leaves, and branches during the harvest. The detachment force between ripe fruit and fruit stalk is the smallest. The results showed that, contrarily to the result of unripe fruit and flower, the fruit-stalk detachment force for ripe fruit was greater than detachment force of stalk-branch. Therefore, when the harvester is used, the ripe fruit is typically harvested without stalk. Ripe fruit without stalk can be used to make dried *L. barbarum* or beverage.

Table 1 Result of detachment force

Item	Measure value/N	Mean value/N	Standard deviation
Fruit-stalk of ripe fruit	0.37-1.51	0.84	0.31
Stalk-branch of ripe fruit	0.73-3.51	2.01	0.73
Fruit-stalk of unripe fruit	1.49-3.29	2.52	0.43
Stalk-branch of unripe fruit	0.72-2.98	1.65	0.53
Flower-stalk	0.49-2.06	1.09	0.43
Stalk-branch of flower	0.56-1.29	0.90	0.19
Leaf-branch	0.85-5.36	2.65	0.96

2.2 Harvester structure and working principle

Figure 2 illustrates the overall structure of the torsion harvester according to the studies on the growth environment and tree characteristics of *L. barbarum*. The device is mainly made up of a DC motor, crank, transmission mechanism, guide mechanism, spindle, vibration head, code wheel, optocoupler speed measuring module, screen, and plastic shell.

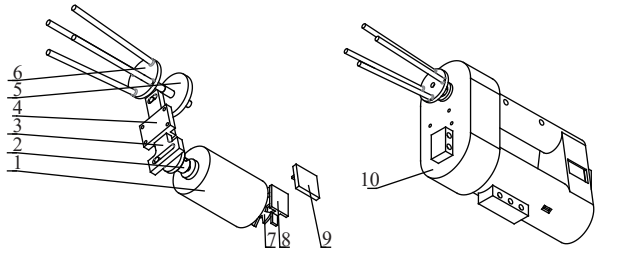

a. Structure b. Appearance

1. DC motor 2. Crank 3. Transmission mechanism 4. Guide mechanism 5. Spindle 6. Vibration head 7. Code wheel 8. Optocoupler speed measuring module 9. Screen 10. Plastic shell

Figure 2 Structure diagram of torsion harvester for *L. barbarum*

When harvesting starts, the handle of the plastic shell is held, the vibrating head is inserted above the ripe fruit, and the branch is positioned between the vibrating rods. When the harvester is turned on, the DC motor drives the crank of the motor to rotate. The guide mechanism limits the movement direction of the transmission mechanism. The crank of the spindle is coaxially and fixedly connected with the vibrating head. The transmission mechanism finally transforms the DC motor's rotation into the reciprocating torsion motion of the vibrating head, which drives the fruit branch to reciprocate. The ripe fruit reciprocates by swinging the branch, and harvesting is realized by inertia force. In addition, the code disk is connected to the DC motor. The DC motor's speed can be measured by the optocoupler speed measuring module, and the vibration frequency can be displayed on the screen in real time. Real-time speed regulation of the entire machine is thus realized.

2.3 Kinematic model

To analyze the torsion harvester, the transmission structure diagram is drawn according to the transmission process as shown in Figure 3a, and the rotation relationship between the vibrating head and the DC motor is simplified as shown in Figure 3b. It can be seen that,

$$l_1 \cos\varphi = l_2 \tag{1}$$

where, l_1 is the distance between the DC motor and the spindle axis, mm; φ is the angle between spindles connecting line and transmission mechanism, (°); and l_2 is the distance between two slots of transmission mechanism, mm.

Implicit equations can be obtained according to geometric relations,

$$r_2 \sin\beta = r_1 \sin\alpha \tag{2}$$

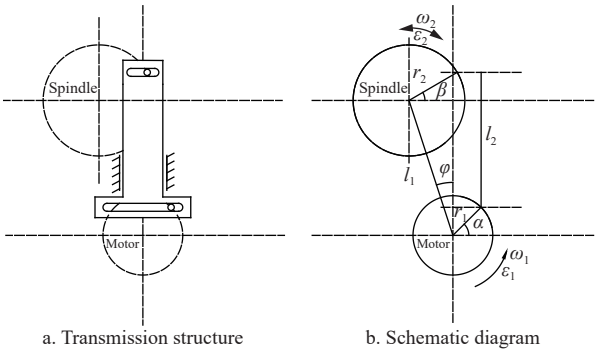

a. Transmission structure b. Schematic diagram

Figure 3 Schematic diagram of transmission structure

where, r_1 is the crank distance, mm; r_2 is the spindle crank distance, mm; α is the crank angle/DC motor angle, (°); and β is the spindle crank angle/vibrating head angle, (°).

Define variable e to simplify Equation (2),

$$e = \frac{r_1}{r_2} \tag{3}$$

Hence, Equation (2) can be simplified as,

$$\sin\beta = e\sin\alpha \tag{4}$$

Find derivatives at both ends of Equation (4),

$$\omega_2 = \frac{e\cos\alpha}{\cos\beta}\omega_1 \tag{5}$$

where, ω_1 is the motor angular velocity, rad/s; ω_2 is the vibration head angular velocity, rad/s.

According to formulas of trigonometric functions, it can be obtained from Equation (4),

$$\cos\beta = \sqrt{1-e^2\sin^2\alpha} \tag{6}$$

Substituting Equation (6) into Equation (5),

$$\omega_2 = \frac{e\omega_1\cos\alpha}{\sqrt{1-e^2\sin^2\alpha}} \tag{7}$$

Find derivatives at both ends of Equation (7),

$$\varepsilon_2 = \frac{e\varepsilon_1\cos\alpha(1-e^2\sin^2\alpha)+e\omega_1^2\sin\alpha(e^2-1)}{(1-e^2\sin^2\alpha)^{\frac{3}{2}}} \tag{8}$$

where, ε_1 is the angular acceleration of DC motor, rad/s^2; ε_2 is the angular acceleration of vibration head, rad/s^2.

Because the DC motor rotates at a uniform speed during harvesting, ε_1=0,

$$\varepsilon_2 = \frac{e\omega_1^2\sin\alpha(e^2-1)}{(1-e^2\sin^2\alpha)^{\frac{3}{2}}} \tag{9}$$

Thus,

$$a = \varepsilon_2 R = \frac{Re\omega_1^2\sin\alpha(e^2-1)}{(1-e^2\sin^2\alpha)^{\frac{3}{2}}} \tag{10}$$

where, a is the tangential acceleration of vibrating rod, m/s^2; R is the distance between vibrating rod and spindle of vibrating head, m.

When the crank of the motor turns to the highest or lowest position in the vertical direction ($\alpha = \pm 90°$), the rotation angle of the vibrating head is turned to the limit, the limit rotation angle of the vibrating head β_{max} can be obtained from the geometric relationship,

$$\beta_{max} = \arcsin e \tag{11}$$

The maximum torsion angle β_r of vibration head can be obtained as,

$$\beta_r = 2\arcsin e \tag{12}$$

2.4 Simulation and analysis based on ADAMS

The models of branch, fruit, and harvester are established in SolidWorks. To simplify the model and improve the simulation efficiency, the harvester model only includes the necessary transmission structure and vibration head. To ensure the accuracy of the simulation test, the branch 3D model was imported into HyperMesh in Parasolid form to make the model flexible. Material parameters and boundary conditions are then defined; the parameters are listed in Table 2. The branch model was divided using a Tetrahedral grid, yielding 8091 nodes and 30 986 units.

The fruits and harvester models are imported into ADAMS software, and the vibration rod and branch are set to come into contact and collide. The fixed constraint is set at the beginning of the branch. According to the characteristics of infinite inflorescence, ripe fruit is near the beginning of the branch whereas the unripe fruit is near its end. The fruit stalk, which is in the form of a flexible connecting rod, joins the fruit to the branches. The crank is driven to rotate at a constant speed and the vibrating rod excites the branch through mechanism transmission. The excitation simulation model is shown in Figure 4.

Table 2 The material mechanics parameters of branch

Item	Measured value
Density/ kg·m^{-3}	556.6
Axial elastic modulus/MPa	509.1
Radial elastic modulus/MPa	45.88
Axial shear modulus/MPa	17.32
Radial shear modulus/MPa	5.92
Axial Poisson's ratio	0.3
Radial Poisson's ratio	0.111

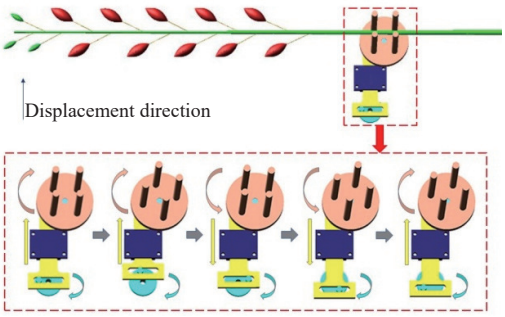

Figure 4 Simulation model

In ADAMS/PostProcessor environment, measuring points were added on ripe and unripe fruits to measure the displacement, velocity, and acceleration during vibration harvesting. The inertia force required for ripe and unripe fruits to fall off can be calculated using the inertia formula. Simulation results show that when the torsion angle (X_1) is 60°-80°, the rods distance (X_2) is 20-30 mm, and the vibration frequency (X_3) is 15-25 Hz, the effect of harvesting ripe fruits while leaving unripe fruits can be realized. Further investigation reveals that, when the torsion angle is 70°, the rods distance is 30 mm, and the vibration frequency is 20 Hz, the comprehensive harvesting effect is better. In the simulation, the displacement, velocity, and acceleration of ripe and unripe fruits was measured, and the graph was displayed by post-processing, as shown in Figure 5, in which the displacement direction is shown in Figure 4.

According to the inertia force formula, calculate the inertia force of ripe fruit and unripe fruit as shown in the Figure 6. The yellow straight line indicates the detachment force of ripe fruit. The blue straight line indicates the detachment force of unripe fruit. During the entire harvesting process, ripe fruit reached the detachment force many times, and the force of unripe fruit was far less than the detachment force, which met the harvesting requirements.

2.5 Parameter optimization experiments

The test has taken place at the location and under the conditions mentioned earlier, on July 6, 2022. The main design requirement of a harvester is to harvest all the ripe fruits without damage and avoid harvesting unripe fruits to the most possible extent to prevent the subsequent yield from being affected. The main purpose of this

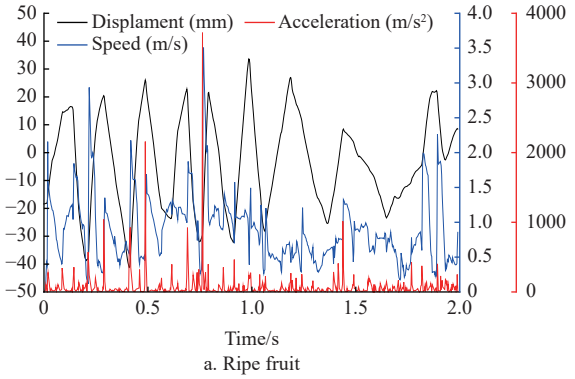

a. Ripe fruit

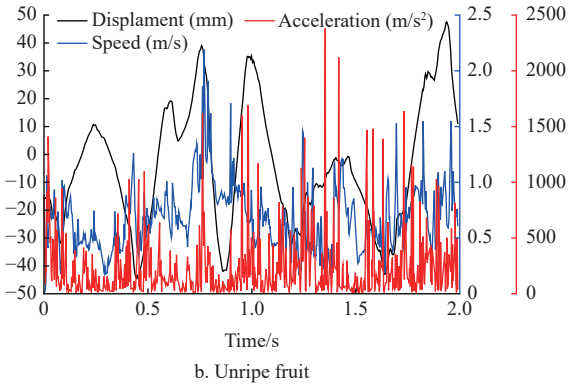

b. Unripe fruit

Figure 5 Fruit vibration response

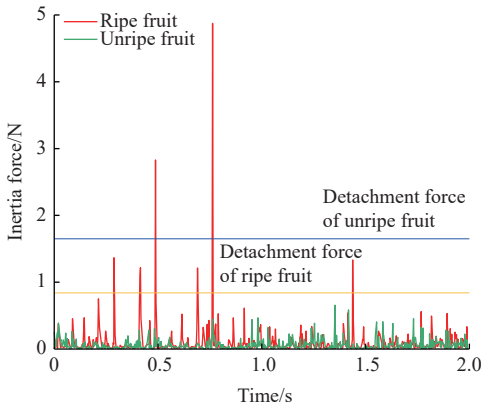

Figure 6 Fruit inertia force

harvester performance test is to investigate the comprehensive harvesting effect. The harvesting rate of ripe fruit (I_1), the harvesting rate of unripe fruit (I_2), and the damage rate of ripe fruit (I_3) were selected as the evaluation indexes for the experiments and calculated according to the following:

$$I_1 = \frac{n_1}{n_1 + n_2} \times 100\% \tag{13}$$

$$I_2 = \frac{n_3}{n_3 + n_4} \times 100\% \tag{14}$$

$$I_3 = \frac{n_5}{n_1} \times 100\% \tag{15}$$

where, n_1 is the amount of harvested ripe fruit; n_2 is the amount of unharvested ripe fruit; n_3 is the amount of harvested unripe fruit; n_4 is the amount of unharvested unripe fruit; and n_5 is the amount of harvested ripe fruit that is damaged.

The scheme adopts three-factor and three-level quadratic orthogonal rotation combination test. The coding factors are listed in Table 3, and the test scheme and results are listed in Table 4. There are 17 groups of experiments, and each group of tests was conducted for 5 times. Design-Expert 12 software was used to complete the test scheme design and result analysis.

Table 3 The codes of factors

Codes	Torsion angle/(°)	Rods distance/mm	Vibration frequency/Hz
–1	60	20	15
0	70	30	20
1	80	40	25

Table 4 The experiment schemes and results

No.	X_1	X_2	X_3	I_1/%	I_2/%	I_3/%
1	–1	–1	0	74.76	1.84	9.09
2	1	–1	0	71.43	5.06	6.67
3	–1	1	0	84.88	3.47	4.11
4	1	1	0	98.08	6.32	2.94
5	–1	0	–1	74.29	0.84	9.62
6	1	0	–1	86.96	1.81	6.67
7	–1	0	1	88.30	6.33	4.82
8	1	0	1	99.04	11.38	1.94
9	0	–1	–1	65.85	0.71	11.11
10	0	1	–1	87.07	2.67	6.93
11	0	–1	1	82.28	4.20	4.62
12	0	1	1	95.73	9.78	3.57
13	0	0	0	90.48	3.28	2.63
14	0	0	0	88.37	6.03	3.95
15	0	0	0	93.51	2.21	4.17
16	0	0	0	96.43	4.76	1.23
17	0	0	0	97.10	4.72	4.48

3 Results and discussion

3.1 Regression analysis of test results

According to the test results, the quadratic regression equation is fitted by Design-Expert 12 software, and the following polynomial regression equation is produced using the harvesting rate of ripe fruit as the response function and the coded values of various factors as independent variables:

$$I_1 = 93.18 + 4.16X_1 + 8.93X_2 + 6.4X_3 + 4.13X_1X_2 - 0.4825X_1X_3 - 1.94X_2X_3 - 3.24X_1^2 - 7.65X_2^2 - 2.79X_3^2 \tag{16}$$

The regression equation is analyzed by variance, as shown in Table 5. The results show that the p value of the regression model is less than 0.05, and the model has statistical significance. Factors X_1, X_2, X_3, X_1X_2, and X_2^2 have significant impact on the harvesting rate of ripe fruit. Other factors are not significant; the p value of the missing term is greater than 0.05, which indicates that there are no missing factors in the regression equation.

In the same way, the following polynomial regression equation is produced, using the harvesting rate of unripe fruit as the response function and the coding value of each factor as the independent variable:

$$I_2 = 4.2 + 1.51X_1 + 1.3X_2 + 3.21X_3 - 0.0925X_1X_2 + 1.02X_1X_3 + 0.905X_2X_3 + 0.3613X_1^2 - 0.3888X_2^2 + 0.5288X_3^2 \tag{17}$$

The regression equation is analyzed by variance, as shown in Table 6. The results show that the p value of the regression model is less than 0.05, and the model has statistical significance. Factors X_1, X_2, X_3 have significant impact on harvesting rate of unripe fruit. Other factors are not significant; the p value of the missing term is greater than 0.05, which indicates that there are no missing factors in the regression equation.

Table 5 Variance analysis of the harvesting rate of ripe fruit

Sources	Sum of Squares	Degree of Freedom	Mean Square	F	p
Model	1539.61	9	171.07	14.96	0.0009
X_1	138.44	1	138.44	12.11	0.0103
X_2	637.96	1	637.96	55.78	0.0001
X_3	327.42	1	327.42	28.63	0.0011
X_1X_2	68.31	1	68.31	5.97	0.0445
X_1X_3	0.9312	1	0.9312	0.0814	0.7836
X_2X_3	15.09	1	15.09	1.32	0.2884
X_1^2	44.14	1	44.14	3.86	0.0902
X_2^2	246.59	1	246.59	21.56	0.0024
X_3^2	32.84	1	32.84	2.87	0.134
Lack of fit	23.59	3	7.86	0.5571	0.6708
Pure error	56.46	4	14.12		
Total	1619.66	16			

Table 6 Variance analysis of the harvesting rate of unripe fruit

Sources	Sum of Squares	Degree of Freedom	Mean Square	F	p
Model	123.95	9	13.77	6.92	0.0092
X_1	18.27	1	18.27	9.18	0.0191
X_2	13.6	1	13.6	6.83	0.0347
X_3	82.3	1	82.3	41.36	0.0004
X_1X_2	0.0342	1	0.0342	0.0172	0.8993
X_1X_3	4.16	1	4.16	2.09	0.1914
X_2X_3	3.28	1	3.28	1.65	0.2403
X_1^2	0.5495	1	0.5495	0.2761	0.6155
X_2^2	0.6363	1	0.6363	0.3198	0.5894
X_3^2	1.18	1	1.18	0.5916	0.467
Lack of fit	5.19	3	1.73	0.7918	0.5586
Pure error	8.74	4	2.18		
Total	137.88	16			

In the same way, the following polynomial regression equation is produced, using the damage rate of ripe fruit as the response function and the coding value of each factor as the independent variable:

$$I_3 = 3.29 - 1.18X_1 - 1.74X_2 - 2.42X_3 + 0.3125X_1X_2 + 0.0175X_1X_3 + 0.7825X_2X_3 + 0.8077X_1^2 + 1.60X_2^2 + 1.66X_3^2 \quad (18)$$

The regression equation is analyzed by variance, as shown in Table 7. The results show that the p value of the regression model is less than 0.05, and the model has statistical significance. Factors X_1, X_2, X_3, X_2^2, and X_3^2 have significant impact on damage rate of ripe fruit. Other factors are not significant; the p value of the missing term is greater than 0.05, which indicates that there are no missing factors in the regression equation.

Table 7 Variance analysis of the damage rate of ripe fruit

Sources	Sum of Squares	Degree of Freedom	Mean Square	F	p
Model	113.02	9	12.56	9.29	0.0038
X_1	11.09	1	11.09	8.21	0.0242
X_2	24.29	1	24.29	17.98	0.0038
X_3	46.95	1	46.95	34.74	0.0006
X_1X_2	0.3906	1	0.3906	0.2891	0.6075
X_1X_3	0.0012	1	0.0012	0.0009	0.9768
X_2X_3	2.45	1	2.45	1.81	0.2202
X_1^2	2.75	1	2.75	2.03	0.1969
X_2^2	10.82	1	10.82	8	0.0254
X_3^2	11.64	1	11.64	8.61	0.0219
Lack of fit	2.15	3	0.7179	0.3931	0.7655
Pure error	7.31	4	1.83		
Total	122.48	16			

3.2 Response surface analysis of test results

By analyzing the influence of various experimental factors on ripe fruit harvesting rate, the regression equation's response surface is shown in Figure 7. As shown in Equation (16) and Table 5, the rods distance has the greatest influence on the harvesting rate of ripe fruit, followed by the vibration frequency and the torsion angle. The interaction between the torsion angle and the rods distance has a significant influence. As shown in Figure 7, the harvesting rate of ripe fruit gradually increases as torsion angle and vibration frequency increase. However, due to structural constraints, it is difficult to further increase the torsion angle and vibration frequency. A further increase could have adverse effects on other evaluation indexes. The harvesting rate of ripe fruit first increases rapidly with the increase in rods distance, and then decreases slowly. This is because the rods distance can improve the vibration intensity by affecting the vibration amplitude. But when the vibration rods distance is too large, the size of the vibrating head is larger than the length of the fruitless area above the ripe fruit growing area. During the harvesting process, some ripe fruits are located inside the vibrating head where the vibration is small. It is therefore challenging to harvest them, in which causes a slight decrease in the harvesting rate of ripe fruit.

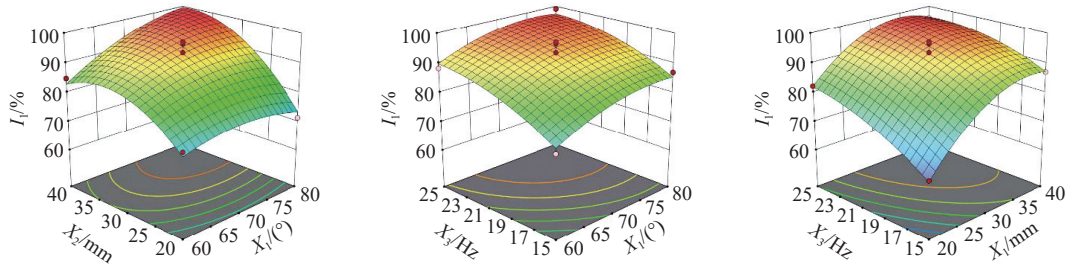

a. Torsion angle and rods distance b. Torsion angle and vibration frequency c. Rods distance and vibration frequency

Figure 7 Response surface of influence of various factors on the harvesting rate of ripe fruit

After analyzing the influence of various experimental factors on the harvesting rate of unripe fruit, the response surface of regression equation is shown in Figure 8. As shown in Equation (17) and Table 5, the factors influencing the harvesting rate of unripe fruit are vibration frequency, torsion angle, and rods distance, from high to low. These factors do not significantly interact. As shown in Figure 8, with the increase in torsion angle, rods distance, and vibration frequency, the harvesting rate of unripe fruit gradually increases. This is because the harvesting rate of unripe fruit is directly related to the vibration intensity. When the

vibration intensity is too high, the inertia force of unripe fruit is greater than the detachment force, resulting in fruits fall off. Additionally, the unripe fruits at the end of branches grow in clusters and the branches are thin. When the vibration intensity is too high, the entire cluster of unripe fruits at the end of branches will fall off, and even the branches will be broken. As a result, the harvesting rate of unripe fruit will rapidly increase. As shown in Table 3, the harvesting rate of unripe fruit is mostly less than 5%, because artificial harvesting can easily control the vibration time. When the ripe fruit area is basically harvested, the harvester will be stopped. Moreover, the vibration area is far away from unripe fruits, thus effectively reducing their shedding.

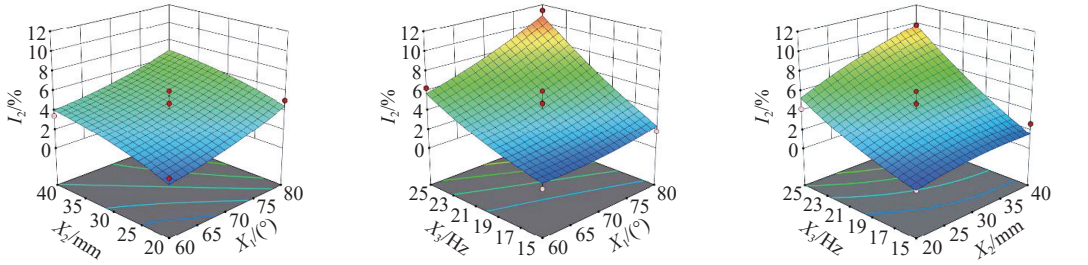

a. Torsion angle and rods distance b. Torsion angle and vibration frequency c. Rods distance and vibration frequency

Figure 8 Response surface of influence of various factors on the harvesting rate of unripe fruit

Figure 9 depicts the response surface of the regression equation for the damage rate of ripe fruit after examining the impact of various experimental factors on that rate. It is clear from Equation (18) and Table 6 that the order of influence on the damage rate of ripe fruit is, from high to low: vibration frequency, rods distance, and torsion angle. Moreover, the interaction of each factor is not significant. As shown in Figure 9, with the increase in torsion angle and vibration frequency, the damage rate of ripe fruit gradually decreases, which is different from the actual harvesting experiment. However, this is because it is difficult to ensure that the fruit will be shaken off without touching it when the vibration intensity is too low. It is common for the vibrating head to be too close to the ripe fruit area, causing the ripe fruit to be struck by the vibrating rod's comb brush and fall off, causing damage to the fruit. As the rods distance increases, the ripe fruit damage decreases rapidly at first, and then increases slowly. This is because the size of vibrating head is too large, which will also cause contact between vibrating rod and ripe fruit. Ripe fruit will be harmed as a result.

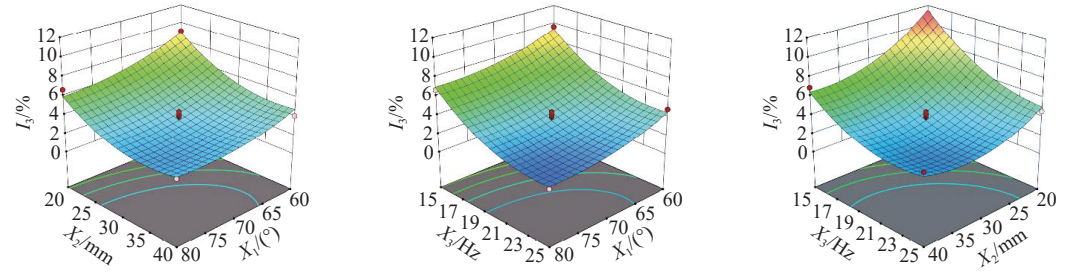

a. Torsion angle and rods distance b. Torsion angle and vibration frequency c. Rods distance and vibration frequency

Figure 9 Response surface of influence of various factors on the damage rate of ripe fruit

3.3 Parameter optimization

Design-Expert 12 software was used to optimize three evaluation indexes: the harvesting rate of ripe fruit (I_1), the harvesting rate of unripe fruit (I_2), and the damage rate of ripe fruit (I_3). The optimization objective equation is shown in Equation (19). Meanwhile, since the main objective of the harvester is to increase the harvesting rate of ripe fruit, the weight distribution ratio of the three evaluation indexes is 4:3:3 determined empirically.

$$I=\begin{cases}\max I_1(X_1,X_2,X_3)\\ \min I_2(X_1,X_2,X_3)\\ \min I_3(X_1,X_2,X_3)\\ 60^\circ \le X_1 \le 80^\circ\\ 20\ \text{mm} \le X_2 \le 40\ \text{mm}\\ 15\ \text{Hz} \le X_3 \le 25\ \text{Hz}\end{cases} \tag{19}$$

The optimal parameter combination for each factor obtained by solving the objective formula is: torsion angle 73.66°, rods distance 35.51 mm, vibration frequency 19.12 Hz.

3.4 Field experiment

The field experiment was conducted on July 10, 2022. The experiment was repeated for 10 times to eliminate random errors. Field experiment results showed that the harvesting rate was 95.67% and 4.68% for ripe and unripe fruits, respectively, and the damage rate of ripe fruit was 3.70%. The harvest experiment is shown in Figure 10.

4 Conclusions

A torsion harvester was designed by studying the characteristics of infinite inflorescence of *L. barbarum* and the detachment force of fruit-flower-leaf-branch. The kinematics and dynamics model of the harvester was established and simulated. The optimized parameters were then obtained and verified. The findings of this study can be summarized as follows:

1) In order to harvest *L. barbarum* with high efficiency, planting agronomy was examined, and the detachment force between ripe fruits, unripe fruits, flowers, leaves and branches was tested. The order of detachment force was then determined.

2) A torsion harvester was designed and the harvester's kinematics model was established based on the characteristics of infinite inflorescence of *L. barbarum* and the detachment force results.

a. Before b. During c. After

Figure 10 Field experiment

3) ADAMS was used to simulate the kinematics and dynamics and test the branch's flexibility. The displacement, speed, and acceleration of ripe and unripe fruit were measured in vibration harvesting. The findings demonstrated that the conditions of harvesting ripe fruits and leaving unripe fruits were met when the rotation angle was 60°-80°, the distance between vibrating rods was 20-30 mm and the vibration frequency was 15-25 Hz.

4) The mathematical model between harvesting rate of ripe fruit, harvesting rate of unripe fruit, damage rate of ripe fruit and torsion angle, vibration rods distance, and vibration frequency was established through an orthogonal combination test using Design-Expert 12 software. The influence of various factors on performance indicators was analyzed, and the best parameter combination was determined: torsion angle 73.66°, vibration rods distance 35.51 mm, and vibration frequency 19.12 Hz. The field experiment showed that the harvesting rates of ripe and unripe fruit is 95.67% and 4.68%, respectively, and the damage rate of ripe fruit is 3.70%.

Acknowledgements

This study was financially supported by the National Natural Science Foundation of China (Grant No. 32272001) and Key Research and Development Program of Ningxia Hui Autonomous Region (Grant No. 2022BBF01002). The authors thank the editors and the anonymous reviewers for their constructive suggestions on the paper.

[References]

[1] Zhao J. Key technologies of vibrating and comb brushing harvesting for *Lycium barbarum* L. Yangling: Northwest A&F University, 2022.

[2] Chen Q Y, Zhang S X, Hu G R, Zhou J G, Zhao J, Chen Y, et al. Parameter optimization of the harvest method in the standardized hedge cultivation mode of *Lycium barbarum* using response surface methodology. Horticulturae, 2022; 8(4): 308.

[3] Zhao J, Chen J. Detecting Maturity in Fresh Lycium barbarum L. Fruit Using Color Information. Horticulturae, 2021; 7(5): 108.

[4] Chen Y, Zhao J, Hu G R, Chen J. Design and Testing of a Pneumatic Oscillating Chinese Wolfberry Harvester. Horticulturae, 2021; 7(8): 214.

[5] Zhao J, Ma T, Inagaki T, Chen Y, Hu G R, Wang Z W, et al. Parameter Optimization of Vibrating and Comb-Brushing Harvesting of Lycium barbarum L. Based on FEM and RSM. Horticulturae, 2021; 7(9): 286.

[6] Li Q, Ye L Q, An W. The suitable working of wolfberry harvest machine. Journal of Agricultural Mechanization Research, 2009; 31(6): 126–128. (in Chinese)

[7] Wang R Y, Zheng Z A, Xu L M, Wu G, Chen J W, Yuan Q C, et al. Simulation and experiment on vibration characteristics of Lycium barbarum falling off. Journal of Agricultural Mechanization Research, 2019; 41(10): 120–128. (in Chinese)

[8] Hu M M, Wan F X, Du X L, Huang X P. Design of vibrating wolfberry picking machine. Journal of Chinese Agricultural Mechanization, 2018; 39(7): 25–29. (in Chinese)

[9] Ma J W. Research status and prospect of the machanized technology of picking wolfberry in China. Mechanical Research & Application, 2017; 30(4): 151–153. (in Chinese)

[10] Zhou B, He J. Design of simulate hand wolfberry picking machine. Transactions of the CSAE, 2010; 26(S1): 13–17. (in Chinese)

[11] Mei S, Xiao H R, Shi Z G, Jiang Q H, Zhao Y, Ding W Q. Design and test of low-loss Lycium barbarum harvesting technology and equipment based on reciprocating vibration method. Journal of Chinese Agricultural Mechanization, 2019; 40(11): 100–105, 208. (in Chinese)

[12] Li L K. Research on the biomechanical characteristic of Woifberry plant based on the Vibrating Harvesting. Ningxia: Ningxia University, 2020.

[13] Zhang W Q, Zhang M M, Zhang J X, Li W. Design and experiment of vibrating wolfberry harvester. Transactions of the CSAM, 2018; 49(7): 97–102. (in Chinese)

[14] Zhang W Q, Li Z Z, Tan Y Z, Li W. Optimal design and experiment on variable pacing combing brush picking device for Lycium barbarum. Transactions of the CSAM, 2018; 49(8): 83–90. (in Chinese)

[15] Xu L M, Chen J W, Wu G, Yuan Q C, Ma S, Yu C C, et al. Design and operating parameter optimization of comb brush vibratory harvesting device for wolfberry. Transactions of the CSAE, 2018; 34(9): 75–82. (in Chinese)

[16] Chen J, Zhao J, Chen Y, Pu L X, Hu G R, Zhang N Y. Design and Experiment on Vibrating and Comb Brushing Harvester for Lycium barbarum. Transactions of the CSAM, 2019; 50(1): 152–161, 95. (in Chinese)

[17] He M, Kan Z, Li C S, Wang L H, Yang L T, Wang Z. Mechanism analysis and experiment on vibration harvesting of wolfberry. Transactions of the CSAE, 2017; 33(11): 47–53. (in Chinese)

[18] Zhang Z, Xiao H R, Ding W Q, Mei S. Mechanism simulation analysis and prototype experiment of *Lycium barbarum* harvest by vibration mode. Transactions of the CSAE, 2015; 31(10): 20–28. (in Chinese)

[19] Erdogan D, Guner M, Dursun E, Gezer I. Mechanical Harvesting of Apricots. Biosystems Engineering, 2003; 85(1): 19–28.

[20] Niu Z J, Zhang X, Deng J, Zhang J, Pan S J, Mu H T. Optimal vibration parameters for olive harvesting from finite element analysis and vibration tests. Biosystems Engineering, 2022; 215(22): 228–238.

[21] Ferreira J R L D G, Silva F M D, Ferrira D D, Souza C E P D, Pinto A W M, Borges F E D M B. Dynamic behavior of coffee tree branches during mechanical harvest. Computers and Electronics in Agriculture, 2020; 173: 105415.

[22] Wu D, Zhao E, Fang D, Jiang S, Wu C, Wang W W, et al. Determination of Vibration Picking Parameters of Camellia oleifera Fruit Based on Acceleration and Strain Response of Branches. Agriculture, 2022; 12(8): 1222.

[23] Du X Q, Shen T F, Zhao L J, Zhang G F, Hu A G, Fang S G, et al. Design and experiment of the comb-brush harvesting machine with variable spacing for oil-tea camellia fruit. Int J Agric & Biol Eng, 2021; 14(1): 172–177.